nature astronomy

Article

https://doi.org/10.1038/s41550-023-02126-2

An abrupt change in the stellar spin-down law at the fully convective boundary

Received: 5 April 2023

Accepted: 10 October 2023

Published online: 13 November 2023



Check for updates

Yuxi (Lucy) Lu 1,2 ×, Victor See 3, Louis Amard4, Ruth Angus 2,5 & Sean P. Matt 66

Unlike partially convective stars such as the Sun, fully convective stars do not possess a radiative core. Whether a star needs this core to generate a solar-like magnetic dynamo is still unclear. Recent studies suggest fully and partially convective stars exhibit very similar period-activity relationships, hinting that dynamos generated by stars with and without radiative cores hold similar properties. Here, using kinematic ages, we discover an abrupt change in the stellar spin-down law across the fully convective boundary. We found that fully convective stars exhibit a higher angular momentum loss rate, corresponding to a torque that is ~1.51 times higher for a given angular velocity than partially convective stars around the fully convective boundary. Because stellar-wind torques depend primarily on large-scale magnetic fields and mass-loss rates, both of which are suggested to be similar for partially and fully convective stars, the observed abrupt change in spin-down law suggests that the dynamos of partially and fully convective stars may be fundamentally different.

The interiors of fully convective (FC) stars $(M < -0.35 M_{\odot})$ and partially convective (PC) stars such as the Sun are fundamentally different. as fully convective stars do not possess a radiative core. How the stellar magnetic dynamo is affected by the existence of a radiative core and the role of the tachocline (the transition region between a star's radiative core and its convective zone) is still unclear. On the observation side, it is well known that the rotation periods and magnetic activities of stars are tightly correlated², and recent observational studies have revealed that stars with different evolutionary stages³ and masses⁴⁻⁶ exhibit similar period-activity relationships, which suggests that all stars obey a universal period-magnetic activity relationship and that a radiative core may not be a critical ingredient for generating a Sun-like dynamo. On the theory side, various dynamo models such as advection-dominated flux transport dynamo models⁷⁻⁹ and turbulent dynamo models¹⁰ can reproduce observations for both partially and fully convective stars to a certain extent, and thus this creates difficulties in understanding the types of dynamo operating in these stars.

One way to break the degeneracy between theoretical predictions and observations is by understanding the time evolution of rotation periods of stars on either side of the fully convective boundary. Because a dynamo is ultimately responsible for generating the surface magnetic fields and the magnetic activity that drives stellar winds, the amount of angular momentum carried away by stellar winds should be sensitive to the details of the dynamo processes. The evolution of rotation rate is sensitive to long-timescale trends in the average wind torque, which thus probes trends in the dipole magnetic field strength and mass-loss rate, both of which should be tied to global dynamo relationships. Therefore, understanding the spin-down law across the fully convective boundary could be the key to revealing the magnetic properties of stars and resolving this discrepancy.

Theoretical rotation evolution models that are constrained by observed rotation period distributions have provided insight into the magnetic topology and angular momentum transport in stars $^{11-14}$. However, most of these works have focused on understanding FGK dwarfs, as both periods and ages for old M dwarfs are extremely difficult

Astronomy Department, Columbia University, New York, NY, USA. Astrophysics Department, American Museum of Natural History, New York, NY, USA. ³European Space Agency (ESA), European Space Research and Technology Centre (ESTEC), Noordwijk, the Netherlands. ⁴AIM, CEA, CNRS, Université Paris-Saclay, Université de Paris, Sorbonne Paris Cité, Gif-sur-Yvette, France. ⁵Center for Computational Astrophysics, Flatiron Institute, New York, NY, USA. ⁶Department of Physics and Astronomy, University of Exeter, Exeter, UK. Se-mail: lucylulu12311@gmail.com

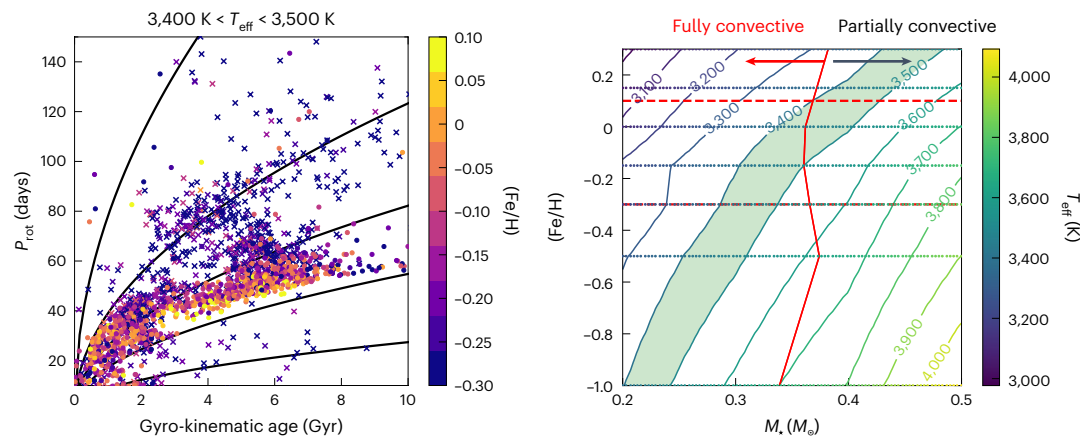


Fig. 1|**Spin-down of stars and stellar models near the fully convective boundary.** Left, observational data showing the $P_{\rm rot}$ –age relationship for stars in the range 3,400 K < $T_{\rm eff}$ < 3,500 K coloured by [Fe/H]. The marker styles show whether a star is determined to be FC (crosses) or PC (circles) using the stellar evolution model shown in the right-hand panel. Right, the fully convective boundary predicted by the STAREVOL ^{22,23} stellar evolution model for stars with various $T_{\rm eff}$ and [Fe/H]. The shaded green area shows the temperature range of the stars in the left-hand panel, and the dotted red lines mark the typical metallicity

range in our sample as shown in the left-hand panel. The model suggests that stars with the same $T_{\rm eff}$ but lower [Fe/H] are fully convective whereas those with higher [Fe/H] are partially convective. Both PC and FC stars should exist between -3,400 K and 3,600 K. The bimodal distribution of rotation periods across stars of different metallicities seen in the left-hand panel suggests that the angular momentum loss rate changes abruptly across the fully convective boundary, in which the FC stars (top sequence; lower [Fe/H]) have a higher angular momentum loss rate compared with the PC stars (bottom sequence; higher [Fe/H]).

to obtain. Old M dwarfs are faint and many rotate slowly (>25 days). This means that photometric data with high sensitivity and a long observational baseline are needed to measure their periods. Ages for old M dwarfs are also hard to infer as their observables change slowly with time, which creates challenges for age dating them with isochrone fitting.

Various studies have provided hints on the spin-down of these low-mass M dwarfs towards older ages. Galactic kinematic and wide binaries on a relatively small sample of M dwarfs with periods obtained from MEarth $^{\rm 15,16}$ found a bimodality of fast and slowly rotating M dwarfs that is difficult to explain with traditional models of angular momentum loss. However, the rotation periods measured for the 4 Gyr open cluster M67 (ref. 17) suggest that old M dwarfs do eventually converge onto a tight sequence. However, we still lack the sample size, especially at older ages, to constrain a spin-down law of these fully convective stars from observational data that can be used to test theoretical models.

A recent catalogue of rotation periods measured using the Zwicky Transient Facility (ZTF) has the sample size needed to understand the spin-down of fully convective stars 18 . With the gyro-kinematic age-dating method 19,20 , we obtained kinematic ages for Kepler and ZTF stars with period measurements (see 'Gyro-kinematic age sample' for more details). We extended the age measurements for fully convective stars up to -10 Gyr and detected an abrupt change in the spin-down law across the fully convective boundary.

Results

A double sequence near the fully convective boundary

The left panel of Fig. 1 shows the rotation period ($P_{\rm rot}$)—age relationship for stars with surface temperature ($T_{\rm eff}$) between 3,400 K and 3,500 K, coloured by metallicity taken from ref. 21. A bimodality emerges in the $P_{\rm rot}$ —age relationship in this temperature range with metal-poor stars spinning down quicker than metal-rich stars.

Stars with similar temperatures can have either fully or partially convective interiors depending on their metallicity. Figure 1 (right-hand plot) shows the fully convective boundary (red line) for stars with different [Fe/H] and temperatures predicted from the STAREVOL stellar evolution model^{22,23} (for details, see 'Stellar evolution model'). We define the fully convective boundary to be the mass at which stars are able to maintain a radiative core after 10 Gyr. Below this threshold,

there is a small range of mass where stars undergo the so-called 'kissing instability' that usually brings them back to a fully convective state after a few cycles²⁴. The model predicts the range of masses for stars that go through 'kissing instability' to be $\sim 0.03 \, M_{\odot}$, and hence the width of the fully convective boundary to be $\sim 0.03 \, M_{\odot}$. Note that we selected the surface temperature of each model at about 5 Gyr. The model suggests that, near the fully convective boundary, stars with the same temperature but lower [Fe/H] are FC whereas those with higher [Fe/H] remain PC, and that both fully and partially convective stars exist between ~3,400 K and 3,600 K. This means that, given a sample of stars with a wide range of [Fe/H] (since the ZTF survey covers the entire northern sky, this statement should be satisfied), we can compare the $P_{\rm rot}$ -age relationship for both fully and partially convective stars with similar masses simultaneously by selecting stars in a narrow range of temperatures near the fully convective boundary. Because the upper sequence in the left-hand plot of Fig. 1 is more metal poor than the lower sequence, we interpret this to mean that the upper sequence consists of FC stars and the lower sequence consists of PC stars. It is also worth pointing out that metallicity measurements are correlated to age, mass and rotation. This means that the separation of the two sequences could be due to factors other than [Fe/H]. However, as shown in the next section, the observable feature in the colour-magnitude diagram (CMD) that is associated with the fully convective boundary and is independent of the metallicity measurements^{24,25} clearly separated the two sequences.

The bimodality of spin-down laws

To further understand whether this bimodality is actually caused by an abrupt change in the spin-down law of stars across the fully convective boundary, we separated the fully and partially convective stars based on their absolute Gaia magnitude, $M_{\rm G}$ and Gaia BP–RP colour measurements using Jao's gap²⁵. We used the Jao gap to separate the stars because the measurements for $M_{\rm G}$ and Gaia BP ($G_{\rm BP}$)—Gaia RP ($G_{\rm RP}$) colour are reliable. Jao's gap is an under-density in the CMD near the fully convective boundary discovered using stars within 200 pc of the Sun from Gaia DR2 (ref. 26). This gap can be approximated by a line connecting ($M_{\rm G}$, $G_{\rm BP}$ – $G_{\rm RP}$) \approx (10.09 mag, 2.35 mag) and ($M_{\rm G}$, $G_{\rm BP}$ – $G_{\rm RP}$) \approx (10.24 mag, 2.55 mag) and is thought to be caused by structural instabilities due to non-equilibrium fusion of ³He (refs. 24,27). In the rest of the paper,

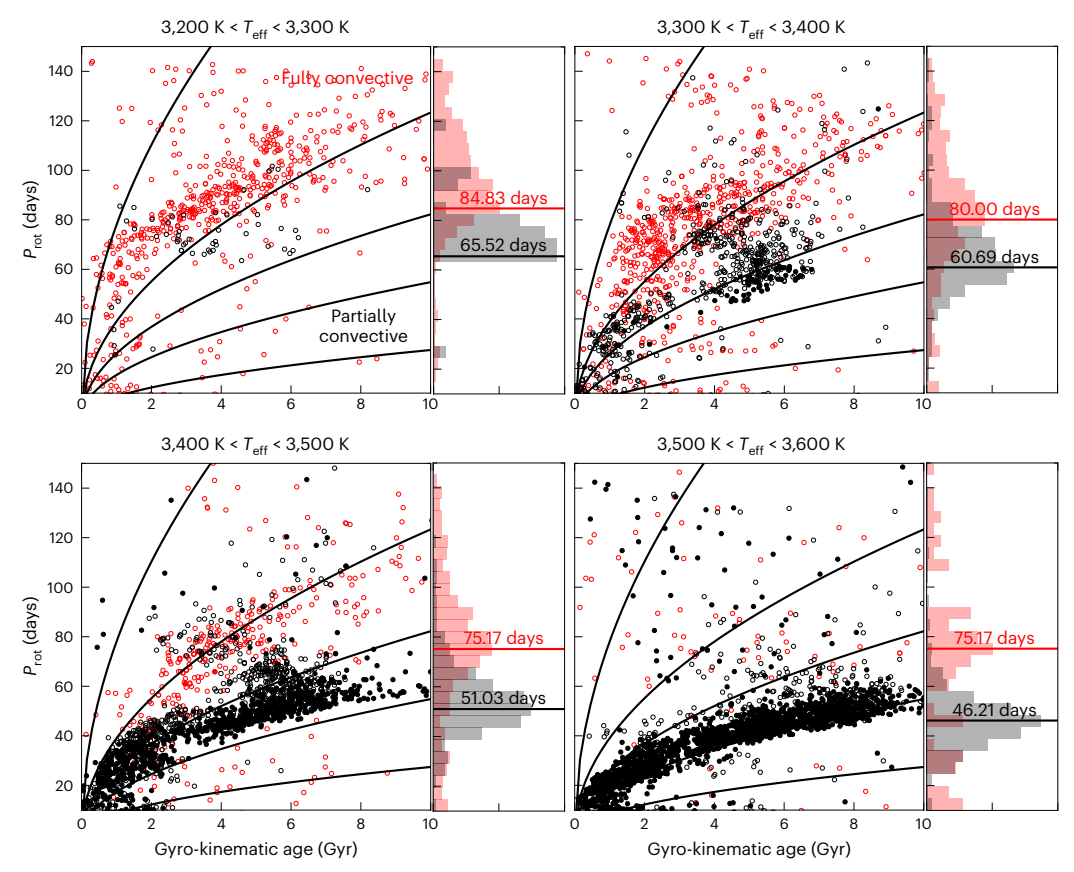


Fig. 2 | **Spin-down sequences for fully and partially convective stars in narrow temperature bins.** $P_{\rm rot}$ -age relationships for stars in four different narrow $T_{\rm eff}$ bins, where the fully convective stars (red) and the partially convective stars (black) are separated using Jao's gap²⁵. The five black lines are Skumanich spindown laws⁵¹ ($P_{\rm rot} \approx {\rm age}^{0.5}$) to guide the eyes. These lines show that, at a given age, the fully convective stars have a spin period that is -1.5 times larger than the

partially convective stars. The marker styles indicate whether the star is fully convective (empty circle) or partially convective (filled circle) based on the STAREVOL stellar evolution model. The normalized histograms (bottom axis ranges from 0 to 0.05) on the right of each subplot are the period distributions for fully convective stars (red) and partially convective stars (black) that have gyro-kinematic ages >2 Gyr.

we use this line to roughly separate the fully and partially convective stars; stars lying above this line in the CMD are more likely to be partially convective and those below are more likely to be fully convective.

We plotted the P_{rot} -age relationship for FC (red) and PC (black) stars in narrow temperature bins of 100 K, between 3,200 K and 3,600 K (Fig. 2). The normalized histograms on the right show the bimodal period distributions of these stars with gyro-kinematic age >2 Gyr and the lines mark the bins with the highest normalized number density. It is notable that the double sequence mostly exists for stars in the range $3,300 \text{ K} < T_{\text{eff}} < 3,500 \text{ K}$: this is slightly lower than, yet very close to, the $T_{\rm eff}$ range that the stellar evolution model predicts to contain both fully and partially convective stars if a sample contains stars with a wide range of [Fe/H] (Fig. 1, right-hand plot). More interestingly, stars below 3,300 K (fully convective) follow the top sequence and those above 3,500 K (partially convective) follow the bottom sequence, which further suggests that the spin-down laws of fully and partially convective stars are bimodal. However, it is worth pointing out that this gap does not provide a clean division between partially and fully convective stars as they can oscillate between this gap while transitioning between being partially and fully convective²⁸.

The abrupt change in the rotational evolution between fully and partially convective stars means that the angular momentum loss rates also exhibit an abrupt change between stars with and without a radiative core. As shown by the detailed calculation in 'Torques for FC and PC stars spinning at the same rate', a fully convective star experiences a higher spin-down torque by a factor of -1.51 than a partially convective star with the same rotation period. Stellar-wind theory then predicts

that, at a given rotation period, fully convective stars should have dipole fields that are -1.26 times stronger or mass-loss rates that are -1.44 times higher (or some combination of both).

The mass dependence of the spin-down laws

With gyro-kinematic ages, we can directly examine the rotation period distributions and spin-evolution isochrones for partially and fully convective stars. We fitted a Markov chain Monte Carlo model using emcee²⁹ by maximizing the log likelihood, calculated by $-0.5 \sum \left(\log_{10} P_{\rm rot} - \log_{10} P_{\rm fit}\right)^2$, where $P_{\rm fit}$ is given by

$$P_{\text{fit}} = 10^{c_1} \tau^{0.5} \left(\frac{M_*}{0.35 M_{\odot}} \right)^{b_1} \frac{\text{days}}{\text{Gyr}^{0.5}} \text{ for } M_* \le M_{\text{FC}}$$
 (1)

$$P_{\text{fit}} = 10^{c_2} \tau^{0.5} \left(\frac{M_*}{0.35 M_{\odot}} \right)^{b_2} \frac{\text{days}}{\text{Gyr}^{0.5}} \text{ for } M_* > M_{\text{FC}}$$
 (2)

where $M_{\rm FC}$ is the mass of the fully convective boundary (-0.35 M_{\circ} based on stellar evolution models), τ is the age of the star in units of billion years and M is the mass of the star in units of M_{\odot} . The best-fitted parameters are $b_1 = -0.770^{0.427}_{-0.363}$, $b_2 = -0.938^{0.448}_{-0.396}$, $c_1 = 1.448^{0.058}_{-0.046}$ and $c_2 = 1.395^{0.029}_{-0.035}M_{\rm FC} = 0.331^{0.015}_{-0.019}M_{\odot}$. The corner plot is shown in Supplementary Fig. 1. It is worth pointing out that the uncertainty for the mass for the fully convective boundary is similar to the range of masses that go through kissing instability predicted from STAREVOL (-0.03 M_{\odot}).

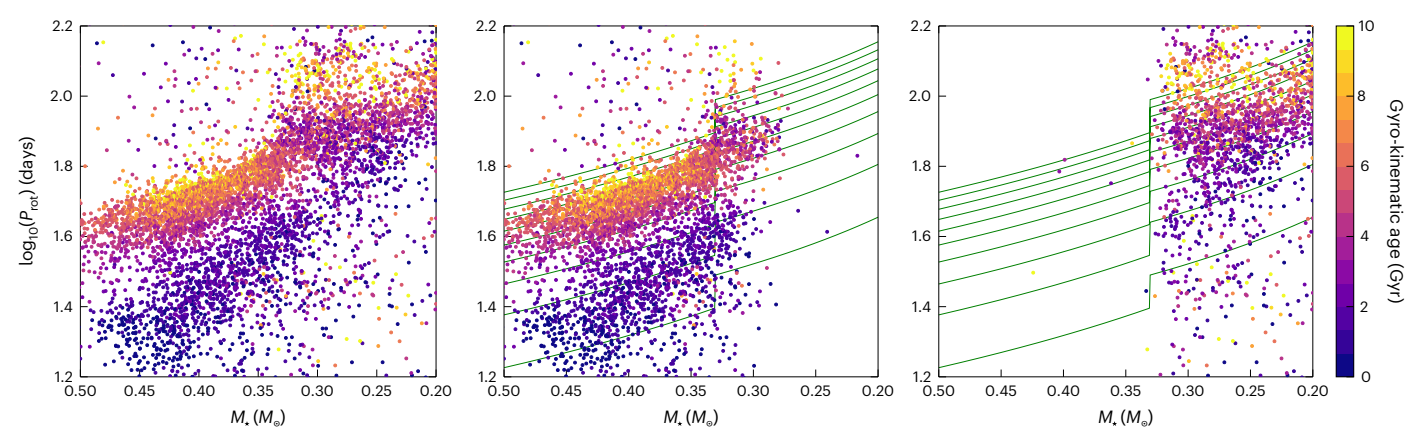


Fig. 3 | Period-mass diagrams plotted with Markov chain Monte Carlo best-fit models. $\log_{10}(P_{\rm rot})$ -mass distribution for the entire sample (left), partially convective stars (middle) and fully convective stars (right) coloured by gyrokinematic ages. The green solid lines are isochrones every 1 Gyr apart from 1 to

 $10~{\rm Gyr}$, derived from equations (1) and (2). The best-fit model suggests that the spin-down law for fully convective stars is slightly more mass dependent than for partially convective stars.

Figure 3 shows the $\log_{10}(P_{rot})$ -mass diagram for all the stars (left), partially convective stars (middle) and fully convective stars (right) coloured by gyro-kinematic ages. The masses are calculated using STAREVOL with metallicity 21 . The green lines show the predicted isochrones every 1 Gyr apart from 0 to 10 Gyr using the model described above.

The intermediate period gap, an observed dearth of stellar rotation periods in the temperature–period diagram at -20 days for G dwarfs and up to -30 days for early-M dwarfs, is believed to be caused by stalling of stars due to core–envelope coupling³⁰. Separating the stars into fully and partially convective shows that this gap appears only in the partially convective stars, which further supports the hypothesis that this period gap is formed from the redistribution of angular momentum between a star's radiative core and its convective envelope, as fully convective stars do not possess a radiative core.

Based on the model fit, the fully convective boundary is at ~0.331 M_{\odot} . The powers of the mass-dependent part of the spin-down law agree within 1σ for fully convective stars and partially convective stars. At the fully convective boundary, fully convective stars spin-down faster than partially convective stars by $[10^{c_1}(M_{FC}/0.35M_{\odot})^{b_1}]/[10^{c_2}(M_{FC}/0.35M_{\odot})^{b_2}] = 1.23$. This gives a 1.51 times higher angular momentum loss rate for fully convective stars, which corresponds to a magnetic field strength that is 1.26 higher, a mass-loss rate that is 1.44 higher or a combination of both 11. For more details, see 'Torques for FC and PC stars spinning at the same rate'.

Discussion

The bimodality of spin-down laws for fully and partially convective stars means that they have fundamentally different spin-down laws and thus different angular momentum loss rates. Observational data suggests that fully convective stars lose angular momentum -1.48 times faster than partially convective stars at a given angular velocity (see 'Torques for FC and PC stars spinning at the same rate' for more details about this calculation). Because stellar spin-down and winds are direct consequences of the stellar dynamo, this suggests that the dynamos of fully convective and partially convective stars are also fundamentally different. This result is pronounced observational evidence that the dynamos of fully convective and partially convective stars operate differently. However, the exact operational difference between their dynamos is not clear, as dynamos and the mechanisms that convert magnetic energy into the heating that drives stellar winds and angular momentum loss are still not well understood.

Typically, stellar-wind theory indicates that the angular momentum loss rate should be directly correlated with the mass-loss rate, and

the strength and geometry of the magnetic fields 31,32 . Observations 33 suggest that the mass-loss rate for fully convective M dwarfs is similar or smaller than that of the Sun based on the ultraviolet spectra of stellar H1Ly α lines from the Hubble Space Telescope. Activity indicators such as X-ray 33 and H α (for example) 5 also suggest that fully and partially convective stars exhibit similar *Ro*-activity relationships, which indicates similar magnetic field strengths. However, our result suggests an abrupt change in the wind torque of only -50% (shown in 'Torques for FC and PC stars spinning at the same rate') and it is not yet clear what may be different in the stellar winds to produce that change and thus whether or not such a change should be visible above the scatter in the observed Rossby number (Ro)-activity relationships.

If the magnetic field strengths are indeed similar, by combining previous studies and this work, we speculate that the differences in the dynamos of fully convective and partially convective stars exist in their magnetic morphology, which causes fully convective stars to generate magnetic dipoles that are stronger but of similar higher-order magnetic fields compared with partially convective stars. Angular momentum loss through magnetic winds (stellar spin-down) is likely to be driven by the escape of open field lines produced by the magnetic dipole ³⁴. The abrupt change in spin-down law across the fully convective boundary discovered in this paper suggests that fully convective stars are likely to have a more poloidal magnetic field configuration than that of partially convective stars.

That fully convective stars might exhibit different dynamos than partially convective stars is also hinted at when looking at fast-rotating M dwarfs³⁵. These fast-rotating, fully convective M dwarfs have either predominantly dipolar, axisymmetric global fields or multipolar, non-axisymmetric dipolar fields.

Methods

Gyro-kinematic age sample

We determined gyro-kinematic ages following the procedure described in ref. 20, where the vertical velocity dispersion for each star was calculated from vertical velocities of stars that are similar in temperature ($T_{\rm eff}$; calculated from $G_{\rm BP}-G_{\rm RP}$ measurements using a polynomial fit taken from ref. 30; $G_{\rm BP}-G_{\rm RP}$ de-reddened using dustmap^{36,37}), rotation periods ($P_{\rm rot}$), absolute Gaia magnitude ($M_{\rm G}$; extinction-corrected using dustmap) and Rossby number (Ro) to the targeted star. The turnover times used to calculate the Rossby number were taken from See et al. (manuscript in preparation) and have the form

$$\tau_{\rm cz} = 0.388 \times 10^{a_1 T_{\rm eff}^2 + a_2 T_{\rm eff} + a_3}$$
 for $T_{\rm eff} \le 3,480 \,\rm K$ (3)

$$\tau_{\rm cz} = 0.388 \times 10^{b_1 T_{\rm eff}^3 + b_2 T_{\rm eff}^2 + b_3 T_{\rm eff} + b_4}$$
 for $T_{\rm eff} > 3,480$ K. (4)

This form was found by fitting polynomials to $\log \tau_{\rm cz}$ and $T_{\rm eff}$ from the stellar structure models²³ at zero age main sequence. The values of the coefficients are $a_1 = 6.5211 \times 10^{-7}$, $a_2 = -4.0036 \times 10^{-3}$, $a_3 = 8.6823$, $b_1 = -2.5190 \times 10^{-10}$, $b_2 = 3.7361 \times 10^{-6}$, $b_3 = -1.8557 \times 10^{-2}$ and $b_4 = 32.5951$.

We then converted the velocity dispersions into stellar ages using an age-velocity-dispersion relationship 38 . Post-main-sequence stars were cut out by only selecting stars with $M_{\rm G}$ > 4.2 mag and equal-mass binaries were excluded by fitting a sixth-order polynomial to the main-sequence stars in $M_{\rm G}$ – $T_{\rm eff}$ space, which moved the fitted polynomial along the $M_{\rm G}$ axis so that it lay directly below the equal-mass binary sequence and removed stars with $M_{\rm G}$ greater than the modified polynomial.

The dataset used in this work is from Lu et al. ³⁹ and combined the ~30,000 stars in ref. 20 from Kepler ⁴⁰ and the ~55,000 stars with period measurements from ref. 18 and Lu et al. ³⁹ from ZTF ⁴¹. The vertical velocities for the ZTF stars were obtained using radial velocity measurements from Gaia DR3 (ref. 42). We did this by transforming from the Solar System barycentric International Celestial Reference System reference frame to Galactocentric Cartesian and cylindrical coordinates using astropy ^{43,44}. The bin size was ($T_{\rm eff}$, $\log_{10}(P_{\rm rot})$, Ro, $M_{\rm G}$) = (177.8 K, 0.15, 0.15, 0.2 mag), optimized following the methodology outlined in ref. 20 using clusters of stars ranging from 0.6 to 4 Gyr (refs. 17,30).

Stellar evolution model

The stellar evolution model for this work was computed using STAREVOL^{22,23}. We used a refined grid of standard models for masses between 0.3 and 0.4 solar masses by steps of 0.01 for eight metallicities between [Fe/H] = -1 and +0.3. Abundances were taken from ref. 45. We used an analytical surface atmospheric fit⁴⁶ and a solar-calibrated mixing length parameter α = 2.11.

Eliminating possible systematic causes

To eliminate the possibility of systematic effects or biases artificially producing this result, we visually examined 100 random ZTF light curves for the fully convective stars between 3,300 K and 3,500 K (where the double spin-down sequence exists) with measured periods >50 days. We found no systematic effect in the measured periods that could cause all the fully convective stars to be on a period harmonic. Moreover, rotation periods in the spin-down sequence for the fully convective stars are not period harmonics (integer multiples) of those for the partially convective stars (Fig. 1). It is also unlikely that a bias or systematic effect in rotation period measurements would conspire to create a double sequence only around the fully convective boundary (Fig. 2) predicted by the stellar evolution model (Fig. 1) and that the CMD gap is able to nicely separate the two sequences (Figs. 2 and 3).

To eliminate the possibility of a systematic effect that could be caused by combining the two data sets from Kepler and ZTF, we performed the same tests with just the ZTF sample with radial velocity measurements from Gaia DR3 and found no notable changes in the results presented in this paper. This is expected, as Kepler mainly targeted solar-like stars and thus provided only 198 stars in the temperature range we are interested in (3,200–3,600 K) compared with 7,809 stars from ZTF. As the number of ZTF stars is more than a magnitude higher than that of Kepler, it is expected that excluding Kepler stars would not affect our results in this study.

Limitations of the gyro-kinematic age-dating method

The gyro-kinematic age-dating technique assumes that stars with similar parameters (effective temperature, rotation period, Rossby number and absolute magnitude) are approximately the same age. In general, it is expected that this assumption should hold. However, if partially convective and fully convective stars have different braking laws, this assumption may be broken for stars near the fully convective boundary. Stars on either side of the boundary, with otherwise

similar properties, could have quite different ages. It is therefore worth examining the behaviour of the gyro-kinematic age-dating method at the fully convective boundary in more detail, given that our results rest upon this technique.

We considered a star near the fully convective boundary: whether it is on the fully or partially convective side of the boundary does not matter. To estimate a gyro-kinematic age for this star, we calculated the vertical velocity dispersion of all the stars contained in a bin in parameter space centred on the star in question and then converted this to an age estimate using an age-velocity-dispersion relationship. Because we are near the fully convective boundary, this bin could contain both fully convective and partially convective stars. If fully convective and partially convective stars do indeed obey different braking laws, then the fully convective and partially convective stars are likely to have different ages even though they are contained within the same bin. The estimated age for the star will therefore be an average age of the fully convective and partially convective populations. This would have the effect of smearing out the sequences in Figs. 1 (left) and 2. The fact that we still see two sequences in these figures, even after this smearing out, suggests that our results are robust to this limitation of the gyro-kinematic age-dating technique. Indeed, in reality, the sequences could be even more well defined than shown in this work.

Torques for FC and PC stars spinning at the same rate

In this section, we determine how much larger the braking torque acting on FC stars is compared with PC stars by considering their observed rotation evolution. At late ages, it is thought that stellar rotation periods increase with the square root of age, which is the well-known Skumanich relationship,

$$P(t) = \alpha t^{0.5},\tag{5}$$

or, in terms of angular frequency,

$$\Omega(t) = \frac{2\pi}{\alpha} t^{-0.5}.$$
(6)

Here, α is a constant of proportionality that we will empirically determine later. The rotation evolution of low-mass stars is governed by the angular momentum equation

$$\frac{\mathrm{d}\Omega}{\mathrm{d}t} = \frac{T}{I} - \frac{\Omega}{I} \frac{\mathrm{d}I}{\mathrm{d}t},\tag{7}$$

where T is the spin-down torque and I is the moment of inertia. On the main sequence, the dI/dt term is approximately zero because a star's stellar structure does not appreciable change during this phase of evolution. Therefore, by differentiating equation (6), substituting into equation (7) and rearranging, one finds that the spin-down torque is given by

$$T = -\frac{\alpha^2 I}{8\pi^2} \Omega^3. \tag{8}$$

The ratio of the torques acting on FC and PC stars, assuming the same angular frequency, is therefore

$$\frac{T_{\rm FC}}{T_{\rm PC}} = \left(\frac{\alpha_{\rm FC}}{\alpha_{\rm PC}}\right)^2 \frac{I_{\rm FC}}{I_{\rm PC}}.\tag{9}$$

For stars at the fully convective boundary $(M_{\bullet} = 0.331 \, M_{\odot})$, $\alpha_{\rm FC}/\alpha_{\rm PC} = 1.23$ (see main text, derived from equations (1) and (2)). As a result, if we consider the case where $I_{\rm FC}/I_{\rm PC} \approx 1$, we find that the ratio of torques is $T_{\rm FC}/T_{\rm PC} \approx 1.23^2 = 1.51$. For this to be the case, stellar-wind theory¹¹ predicts that fully convective stars should have dipole field strengths that are larger by a factor of ~1.26, mass-loss rates that are ~1.44 times larger or

some combination of both of these factors. Further observations are needed to determine which of these scenarios is true.

Data availability

The data used are available in Supplementary Data 1.

References

- Chabrier, G. & Baraffe, I. Structure and evolution of low-mass stars. Astron. Astrophys. 327, 1039–1053 (1997).
- Pallavicini, R. et al. Relations among stellar X-ray emission observed from Einstein, stellar rotation and bolometric luminosity. Astrophys. J. 248, 279–290 (1981).
- Lehtinen, J. J., Spada, F., Käpylä, M. J., Olspert, N. & Käpylä, P. J. Common dynamo scaling in slowly rotating young and evolved stars. Nat. Astron. 4, 658–662 (2020).
- Stelzer, B., Damasso, M., Scholz, A. & Matt, S. P. A path towards understanding the rotation-activity relation of M dwarfs with K2 mission, X-ray and UV data. Mon. Not. R. Astron. Soc. 463, 1844–1864 (2016).
- Newton, E. R. et al. The Hα emission of nearby M dwarfs and its relation to stellar rotation. Astrophys. J. 834, 85 (2017).
- Wright, N. J. et al. The stellar rotation-activity relationship in fully convective M dwarfs. Mon. Not. R. Astron. Soc. 479, 2351–2360 (2018).
- Babcock, H. W. The topology of the Sun's magnetic field and the 22-year cycle. Astrophys. J. 133, 572 (1961).
- Leighton, R. B. A magneto-kinematic model of the solar cycle. Astrophys. J. 156, 1–26 (1969).
- Cameron, R. H. & Schüssler, M. An update of Leighton's solar dynamo model. Astron. Astrophys. 599, A52 (2017).
- Warnecke, J. et al. Investigating global convective dynamos with mean-field models: full spectrum of turbulent effects required. Astrophys. J. Lett. 919, L13 (2021).
- 11. Matt, S. P. et al. The mass-dependence of angular momentum evolution in Sun-like stars. *Astrophys. J. Lett.* **799**, L23 (2015).
- Saders, J. L. et al. Weakened magnetic braking as the origin of anomalously rapid rotation in old field stars. *Nature* 529, 181–184 (2016).
- Garraffo, C. et al. The revolution revolution: magnetic morphology driven spin-down. Astrophys. J. 862, 90 (2018).
- Spada, F. & Lanzafame, A. C. Competing effect of wind braking and interior coupling in the rotational evolution of solar-like stars. Astron. Astrophys. 636, A76 (2020).
- Irwin, J. et al. On the angular momentum evolution of fully convective stars: rotation periods for field M-dwarfs from the MEarth transit survey. Astrophys. J. 727, 56 (2011).
- Berta, Z. K. et al. Transit detection in the MEarth survey of nearby M dwarfs: bridging the clean-first, search-later divide. Astrophys. J. 144, 145 (2012).
- Dungee, R. et al. A 4 Gyr M-dwarf gyrochrone from CFHT/ MegaPrime monitoring of the open cluster M67. Astrophys. J. 938, 118 (2022).
- 18. Lu, Y. et al. Bridging the gap—the disappearance of the intermediate period gap for fully convective stars, uncovered by new ZTF rotation periods. *Astrophys. J.* **164**, 251 (2022).
- Angus, R. et al. Exploring the evolution of stellar rotation using galactic kinematics. Astrophys. J. 160, 90 (2020).
- Lu, Y. et al. Gyro-kinematic ages for around 30,000 Kepler stars. Astrophys. J. 161, 189 (2021).
- Andrae, R., Rix, H.-W. & Chandra, V. Robust data-driven metallicities for 175 million stars from Gaia XP spectra. Astrophys. J. Suppl. Ser. 267, 8 (2023).
- Siess, L., Dufour, E. & Forestini, M. An internet server for pre-main sequence tracks of low- and intermediate-mass stars. Astron. Astrophys. 358, 593–599 (2000).

- 23. Amard, L. et al. First grids of low-mass stellar models and isochrones with self-consistent treatment of rotation. From 0.2 to 1.5 M_{\odot} at seven metallicities from PMS to TAMS. *Astron. Astrophys.* **631**, A77 (2019).
- 24. Saders, J. L. & Pinsonneault, M. H. An ³He-driven instability near the fully convective boundary. *Astrophys. J.* **751**, 98 (2012).
- 25. Jao, W.-C., Henry, T. J., Gies, D. R. & Hambly, N. C. A gap in the lower main sequence revealed by Gaia data release 2. *Astrophys. J. Lett.* **861**, L11 (2018).
- 26. Gaia Collaboration et al. Gaia data release 2. Summary of the contents and survey properties. *Astron. Astrophys.* **616**, A1 (2018).
- Feiden, G. A., Skidmore, K. & Jao, W.-C. Gaia gaps and the physics of low-mass stars. I. The fully convective boundary. *Astrophys. J.* 907, 53 (2021).
- Baraffe, I. & Chabrier, G. A closer look at the transition between fully convective and partly radiative low-mass stars. Astron. Astrophys. 619, A177 (2018).
- 29. Foreman-Mackey, D., Hogg, D. W., Lang, D. & Goodman, J. emcee: the MCMC hammer. *Publ. Astron. Soc. Pac.* **125**, 306 (2013).
- Curtis, J. L. et al. When do stalled stars resume spinning down? Advancing gyrochronology with Ruprecht 147. Astrophys. J. 904, 140 (2020).
- Mestel, L. Angular momentum loss during pre-main sequence contraction. in Cool Stars, Stellar Systems, and the Sun. Lecture Notes in Physics (eds Baliunas, S. L. & Hartmann, L.) Vol. 193, 49 (Springer, Berlin, Heidelberg, 1984).
- 32. Finley, A. J. & Matt, S. P. The effect of combined magnetic geometries on thermally driven winds. II. Dipolar, quadrupolar, and octupolar topologies. *Astrophys. J.* **854**, 78 (2018).
- 33. Wood, B. E. et al. New observational constraints on the winds of M dwarf stars. *Astrophys. J.* **915**, 37 (2021).
- See, V., Lehmann, L., Matt, S. P. & Finley, A. J. How much do underestimated field strengths from Zeeman–Doppler imaging affect spin-down torque estimates? *Astrophys. J.* 894, 69 (2020).
- 35. Kochukhov, O. & Shulyak, D. Magnetic field of the eclipsing M-dwarf binary YY Gem. Astrophys. J. **873**, 69 (2019).
- Green, G. M. dustmaps: a Python interface for maps of interstellar dust. J. Open Source Softw. 3, 695 (2018).
- Green, G. M. et al. Galactic reddening in 3D from stellar photometry—an improved map. Mon. Not. R. Astron. Soc. 478, 651–666 (2018).
- Yu, J. & Liu, C. The age-velocity dispersion relation of the Galactic discs from LAMOST-Gaia data. Mon. Not. R. Astron. Soc. 475, 1093–1103 (2018).
- Lu, Y., Angus, R., Foreman-Mackey, D. & Hattori, S. In this day and age: an empirical gyrochronology relation for partially and fully convective single field stars. Preprint at https://arxiv.org/ abs/2310.14990 (2023).
- 40. Borucki, W. J. et al. Kepler planet-detection mission: introduction and first results. *Science* **327**, 977–980 (2010).
- Bellm, E. C. et al. The Zwicky Transient Facility: system overview, performance, and first results. *Publ. Astron. Soc. Pac.* 131, 018002 (2019).
- 42. Collaboration, G. Gaia data release 3: summary of the content and survey properties. *Astron. Astrophys.* **674**, A1 (2023).
- Collaboration, A. Astropy: a community Python package for astronomy. Astron. Astrophys. 558, A33 (2013).
- Price-Whelan, A. M. et al. The Astropy project: building an open-science project and status of the v2.0 core package. *Astrophys. J.* 156, 123 (2018).
- 45. Asplund, M., Amarsi, A. M. & Grevesse, N. The chemical make-up of the Sun: a 2020 vision. *Astron. Astrophys.* **653**, A141 (2021).
- Krishna Swamy, K. S. Profiles of strong lines in K-dwarfs. Astrophys. J. 145, 174–194 (1966).

- Pordes, R. et al. The open Science grid. J. Phys. Conf. Ser. 78, 012057 (2007).
- 48. Sfiligoi, I. et al. The pilot way to grid resources using glideinWMS. In 2009 WRI World Congress on Computer Science and Information Engineering Vol. 2, 428–432 (IEEE, 2009).
- Ochsenbein, F., Bauer, P. & Marcout, J. The VizieR database of astronomical catalogues. Astron. Astrophys. Suppl. 143, 23–32 (2000).
- Wenger, M. et al. The SIMBAD astronomical database. The CDS reference database for astronomical objects. Astron. Astrophys. Suppl. 143, 9–22 (2000).
- Skumanich, A. Time scales for CA II emission decay, rotational braking, and lithium depletion. Astrophys. J. 171, 565–567 (1972).

Acknowledgements

Y.L. acknowledges support from the the European Space Agency (ESA) through the Science Faculty of the European Space Research and Technology Centre (ESTEC). V.S. acknowledges support from the ESA as an ESA Research Fellow. R.A. acknowledges support from NSF AAG grant no. 2108251. S.P.M. acknowledges support as a visiting scholar from the Center for Computational Astrophysics at the Flatiron Institute, which is supported by the Simons Foundation. This work has made use of data from the ESA mission Gaia, processed by the Gaia Data Processing and Analysis Consortium (DPAC). Funding for the DPAC has been provided by national institutions, in particular, the institutions participating in the Gaia Multilateral Agreement. This research also made use of public auxiliary data provided by ESA/ Gaia/DPAC/CU5 and prepared by Carine Babusiaux. This research was done using services provided by the OSG Consortium^{47,48}, which is supported by the National Science Foundation award nos. 2030508 and 1836650. This research has also made use of NASA's Astrophysics Data System and the VizieR⁴⁹ and SIMBAD⁵⁰ databases, operated at CDS, Strasbourg, France.

Author contributions

Y.L. developed the initial idea and prepared the observational data. L.A. prepared the stellar evolution model. Y.L., V.S., L.A. and R.A. conducted the data analysis. Y.L., V.S., L.A., R.A. and S.P.M. interpreted the broader context and wrote the manuscript.

Competing interests

The authors declare no competing interests.

Additional information

Supplementary information The online version contains supplementary material available at https://doi.org/10.1038/s41550-023-02126-2.

Correspondence and requests for materials should be addressed to Yuxi (Lucy) Lu.

Peer review information *Nature Astronomy* thanks Maarit Korpi-Lagg and the other, anonymous, reviewer(s) for their contribution to the peer review of this work.

Reprints and permissions information is available at www.nature.com/reprints.

Publisher's note Springer Nature remains neutral with regard to jurisdictional claims in published maps and institutional affiliations.

Springer Nature or its licensor (e.g. a society or other partner) holds exclusive rights to this article under a publishing agreement with the author(s) or other rightsholder(s); author self-archiving of the accepted manuscript version of this article is solely governed by the terms of such publishing agreement and applicable law.

@ The Author(s), under exclusive licence to Springer Nature Limited 2023